International Journal of Radiation Oncology biology • physics

www.redjournal.org

Physics Contribution

Tumor Tracking Method Based on a Deformable 4D CT Breathing Motion Model Driven by an External Surface Surrogate

Aurora Fassi, PhD,[*] Joël Schaerer, PhD,[†,‡] Mathieu Fernandes, PhD,[†,‡] Marco Riboldi, PhD,[*,§] David Sarrut, PhD,[†,‡] and Guido Baroni, PhD[*,§]

**Dipartimento di Elettronica, Informazione e Bioingegneria, Politecnico di Milano, Milano, Italy; [†]CREATIS, CNRS UMR 5220, INSERM U1044, Université Lyon 1, INSA-Lyon, Villeurbanne, France; [‡]Department of Radiotherapy, Centre Léon Bérard, Lyon, France; and [§]Bioengineering Unit, CNAO Foundation, Pavia, Italy*

Received Jul 17, 2013, and in revised form Aug 26, 2013. Accepted for publication Sep 13, 2013.

Summary

We report a tumor tracking method for intrafraction moving lesions based on a patient-specific adaptive breathing motion model, which is estimated a priori from time-resolved planning CT images. At each treatment fraction, model parameters are updated relying on in-room radiography acquisition and optical surface imaging. The proposed approach was evaluated on 7 lung cancer patients, obtaining a median tumor tracking accuracy of 1.5 mm in each spatial direction.

Purpose: To develop a tumor tracking method based on a surrogate-driven motion model, which provides noninvasive dynamic localization of extracranial targets for the compensation of respiration-induced intrafraction motion in high-precision radiation therapy.

Methods and Materials: The proposed approach is based on a patient-specific breathing motion model, derived a priori from 4-dimensional planning computed tomography (CT) images. Model parameters (respiratory baseline, amplitude, and phase) are retrieved and updated at each treatment fraction according to in-room radiography acquisition and optical surface imaging. The baseline parameter is adapted to the interfraction variations obtained from the daily cone beam (CB) CT scan. The respiratory amplitude and phase are extracted from an external breathing surrogate, estimated from the displacement of the patient thoracoabdominal surface, acquired with a noninvasive surface imaging device. The developed method was tested on a database of 7 lung cancer patients, including the synchronized information on internal and external respiratory motion during a CBCT scan.

Results: About 30 seconds of simultaneous acquisition of CBCT and optical surface images were analyzed for each patient. The tumor trajectories identified in CBCT projections were used as reference and compared with the target trajectories estimated from surface displacement with the a priori motion model. The resulting absolute differences between the reference and estimated tumor motion along the 2 image dimensions ranged between 0.7 and 2.4 mm; the measured phase shifts did not exceed 7% of the breathing cycle length.

Conclusions: We investigated a tumor tracking method that integrates breathing motion information provided by the 4-dimensional planning CT with surface imaging at the time of treatment, representing an alternative approach to point-based external−internal correlation models. Although an in-room radiograph-based assessment of the reliability of the motion model is envisaged, the developed technique does not involve the estimation and continuous update of correlation parameters, thus requiring a less intense use of invasive imaging.

Reprint requests to: Aurora Fassi, PhD, Dipartimento di Elettronica, Informazione e Bioingegneria, Politecnico di Milano, Piazza Leonardo da Vinci, 32, 20133, Milan, Italy. Tel: (+39) 02-2399-9022; E-mail: aurora.fassi@mail.polimi.it

J.S. is currently at BioClinica SAS, Bioparc, Adenine Building, Lyon, France.

M.F. is currently at: CYTOO SA, Grenoble, France.

Conflict of interest: none.

Int J Radiation Oncol Biol Phys, Vol. 88, No. 1, pp. 182−188, 2014
0360-3016/$ - see front matter
http://dx.doi.org/10.1016/j.ijrobp.2013.09.026

Introduction

The issue of intrafraction organ motion is becoming increasingly important in high-precision extracranial radiation therapy and even more demanding in charged particle therapy because it severely frustrates the accuracy and effectiveness of radiation dose delivery (1, 2). The most relevant source of intrafraction motion is respiration, which affects tumors in the thorax and abdomen, such as lung, liver, and pancreas cancer. Different methodologies have been proposed to compensate for the geometric uncertainties that result from intrafraction organ motion. The most efficient motion-compensated strategy for continuous irradiation in free-breathing is real-time tumor tracking, which is based on the dynamic steering of the radiation beam according to the instantaneous target position (3).

Tumor localization, required for tracking techniques, can be achieved through direct or indirect approaches (1). Direct localization methods rely on the imaging of the lesion or of implanted clips by means of in-room radiography imaging systems. Even if the direct approach can be very accurate (4, 5), its invasiveness because of ionizing radiation restricts the applicability to a limited temporal window of the treatment session. Conversely, indirect localization methods infer target motion from respiratory surrogates, such as the displacement of the thoracoabdominal surface. Noninvasive optical tracking devices can be used to acquire external surface motion by reconstructing the trajectory of passive markers placed on the patient skin (6) or through the markerless imaging of the entire surface (7). The noninvasiveness of this approach allows the continuous monitoring of intrafraction organ motion during the whole treatment course. However, the use of external surrogates to predict target position entails the definition of appropriate external−internal correlation models, which need to be frequently verified to cope with intrafraction modifications of respiratory patterns and to reduce residual uncertainties (8, 9).

In conventional photon radiation therapy, indirect tumor tracking techniques have been already introduced in clinical practice with commercially available solutions (10, 11). Tumor localization is obtained by combining optical tracking of multiple surface markers with x-ray imaging of internal anatomy (12). In case of low-contrast lesions, such as in the liver or lung, radiopaque clips are usually implanted near the tumor to facilitate its detection in radiograph projections. The external−internal correlation model is initialized before treatment by simultaneously acquiring optical surface displacement and x-ray-based target motion. Radiography imaging is also periodically captured throughout the whole treatment duration, typically every 1-2 minutes, to continuously update the correlation model. The external−internal correlation accuracy, assessed in retrospective clinical studies, proved to be within 2.5 mm in the anteroposterior direction and 1.9 mm in the superoinferior and mediolateral directions (13, 14). Errors in target position estimation were reported to vary greatly as a function of breathing irregularities (0.5-11.3 mm range), with a reduction above 6 mm when using correlation models with a higher level of complexity than linear−polynomial correlation (15).

The aim of this study is to develop and investigate an alternative approach for indirect tumor tracking, which does not require the estimation and verification of external−internal correlation parameters. The proposed technique relies on a breathing motion model derived a priori from time-resolved planning computed tomography (CT) and driven during treatment by a respiratory surrogate obtained from markerless surface imaging.

Methods and Materials

Tumor tracking technique

The proposed tumor tracking approach is based on the integration of different imaging modalities, which are conventionally operated in extracranial radiation therapy treatments, such as *(1)* time-resolved planning CT; *(2)* in-room radiography imaging systems; and *(3)* optical devices for dynamic surface imaging. As illustrated in Figure 1, the developed method relies on a patient-specific breathing motion model, which is estimated from the 4-dimensional (4D) CT images acquired for treatment planning. The a priori motion model describes the anatomical changes because of breathing over the entire respiratory cycle and is parameterized as a function of 3 main parameters: baseline, amplitude, and phase. The respiratory baseline is described by the midposition (MidP) CT image, consisting of a time-weighted average of all 4D CT phase volumes (16). Similarly to previous works (17-19), the motion model is expressed in terms of the deformation vector fields obtained by applying B-spline deformable image registration (20) between the MidP image and each 4D CT phase, focusing on a volume of interest around the tumor.

As depicted in Figure 1, the 4D CT motion model is updated at each treatment session according to the anatomical and motion information obtained from in-room radiography imaging and optical surface systems, to compensate for the inter- and intrafraction variations (21, 22). Baseline shifts between treatment planning and the daily treatment session are corrected by nonrigidly registering (20) the MidP image on the free-breathing cone beam (CB)CT volume acquired for patient setup verification, thus generating an adapted baseline image. The updated tumor positions at each phase of the 4D CT breathing cycle are obtained by mapping the adapted baseline according to the deformation vector fields of the a priori motion model (Figure 2a). The breathing amplitude and phase parameters are retrieved from the displacement of the patient external surface, which is continuously acquired during dose delivery by means of noninvasive optical imaging devices. The intersection of the optical surfaces with the patient portion scanned in the planning CT is tracked as region of interest, including the thorax and the upper part of the abdomen.

Because markerless surface models provided by optical tracking systems lack spatial correspondence, a deformable mesh registration algorithm, based on a locally affine regularization, is applied to extract the 3-dimensional (3D) trajectories of corresponding surface points, as described elsewhere (23). For each registered point, a monodimensional motion signal is obtained by computing the time series of the 3D distance from its most posterior position occurred during the optical surface acquisition. The motion trajectories of all surface points in the thoracoabdominal region of interest are then summarized in a single breathing surrogate signal through k-means clustering techniques (24). The respiratory surrogate is obtained by averaging the signal of the first 2 clusters associated to the patient thorax and abdomen to take into account both the thoracic and the abdominal breathing patterns. The instantaneous values of the respiratory amplitude and phase parameters associated to each optical surface image are then estimated from the extracted breathing surrogate.

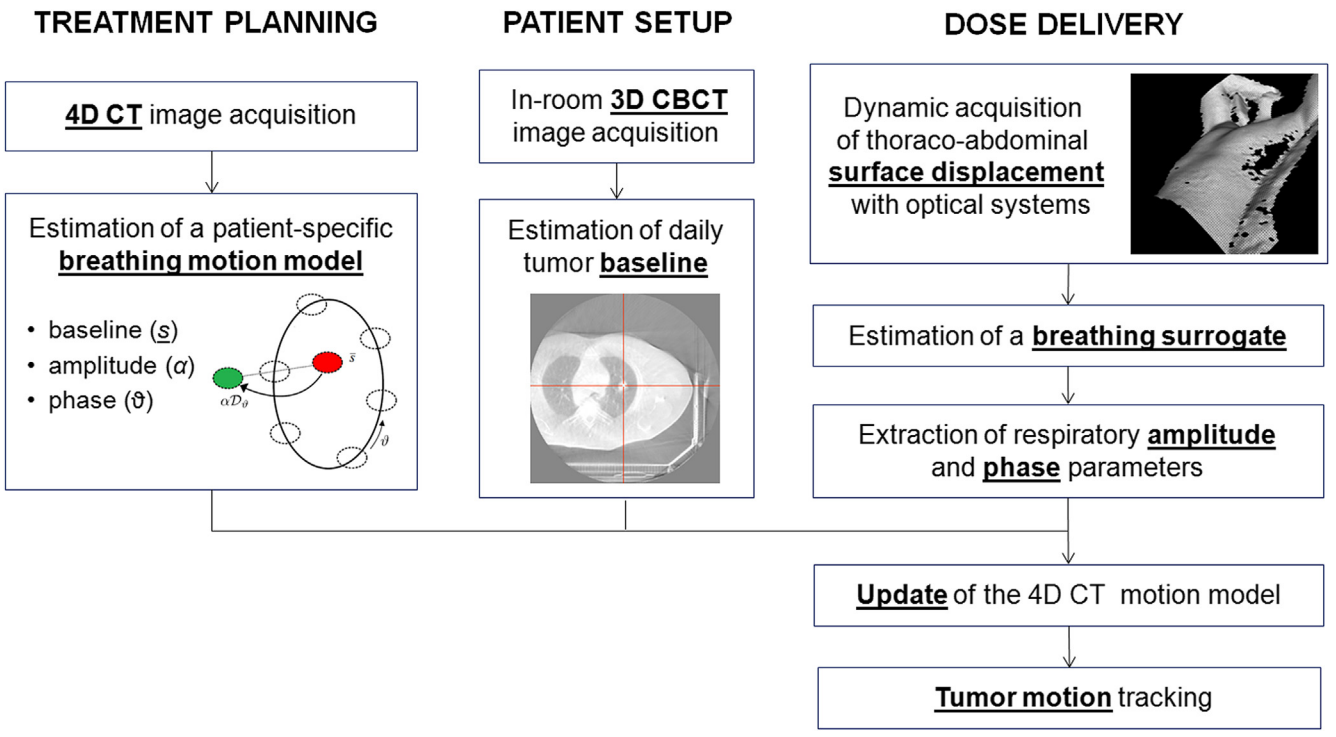

Fig. 1. Schematic representation of the proposed tumor tracking method (the representation of the motion model was extracted from previous work (19)). 3D = 3-dimensional; 4D = 4-dimensional; CT = computed tomography; CBCT = cone beam CT.

To compensate for possible differences in respiratory motion patterns between planning and treatment sessions (25), the displacement of the patient surface optically acquired during treatment is compared to surface motion exhibited during the 4D CT scan. The triangulated meshes corresponding to the thoracoabdominal surface region are extracted from each 4D CT phase image. Deformable mesh registration and k-means clustering are applied to the triangulated 4D CT surfaces to obtain the breathing surrogate during the planning scan. For both treatment and planning surrogate signals, the phase angles of the corresponding analytic signal obtained through Hilbert transform (26) are computed. As shown in Figure 2b, the respiratory phase parameter associated to each optical surface image acquired during treatment is estimated as the interpolated percentage position between 4D CT frames that corresponds to the same phase angle. The breathing amplitude is parameterized according to a scaling factor, computed as the ratio between the amplitudes of treatment and planning surrogate signals at corresponding phase angles. The estimated breathing parameters are then integrated to the a priori 4D CT breathing motion model to obtain the 3D tumor trajectory during the whole course of surface acquisition (Figure 2c). Target coordinates associated to each surface frame are obtained by linearly interpolating the updated tumor positions of the 4D CT motion model at the instantaneous value of the phase parameter. The vector difference between the interpolated lesion coordinates and the adapted tumor baseline is then multiplied by the amplitude scaling factor to amplify or reduce tumor motion with respect to the planning CT scan.

Experimental testing

The developed tumor tracking approach was tested on a clinical database of 7 early-stage non-small cell lung cancer patients with upper-lobe tumors, treated with stereotactic body radiation therapy at Centre Léon Bérard, Lyon, France. Data collected for each patient include a 10-phase 4D CT image set acquired with the Philips Brilliance CT Big Bore scanner (Philips Medical Solution, Cleveland, OH) and the synchronized information on internal−external breathing motion acquired during a CBCT scan (Elekta Synergy System, Elekta, Crawley, UK). For each patient, the displacement of the thoracoabdominal surface was continuously captured with the GateCT optical system (Vision RT, London, UK) during the first 120° of CBCT rotation. For the remaining projection angles, in fact, the rotating gantry and CBCT units occluded the patient surface to the GateCT imaging pod, suspended from the room ceiling on the right side of the treatment couch. CBCT projections were acquired with a frequency of about 5.5 Hz, whereas the acquisition speed of the optical surface images varied from 7.9 and 9.1 Hz, depending on the number of reconstructed surface points. CBCT and GateCT data acquisitions were synchronized in order to retrieve the temporal correspondence between 2-dimensional projections and optical surface images.

The accuracy of the proposed tumor tracking method was evaluated by comparing the reference target trajectory directly identified in CBCT projections with the lesion trajectory estimated from the external surface motion combined with the a priori 4D CT model. The position of lung tumors in CBCT images was identified through the method described previously (27), based on template matching algorithms applied to contrast-enhanced projections. A similar approach for target detection in CBCT images showed a tracking accuracy of about 1 mm in moving phantoms and 2 mm in lung cancer patients (28). To increase target identification rates and accuracy, a manual refinement of the automatically detected lesion coordinates was added by overlying and manually translating on the contrast-enhanced images the tumor contours projected at the corresponding angle. The

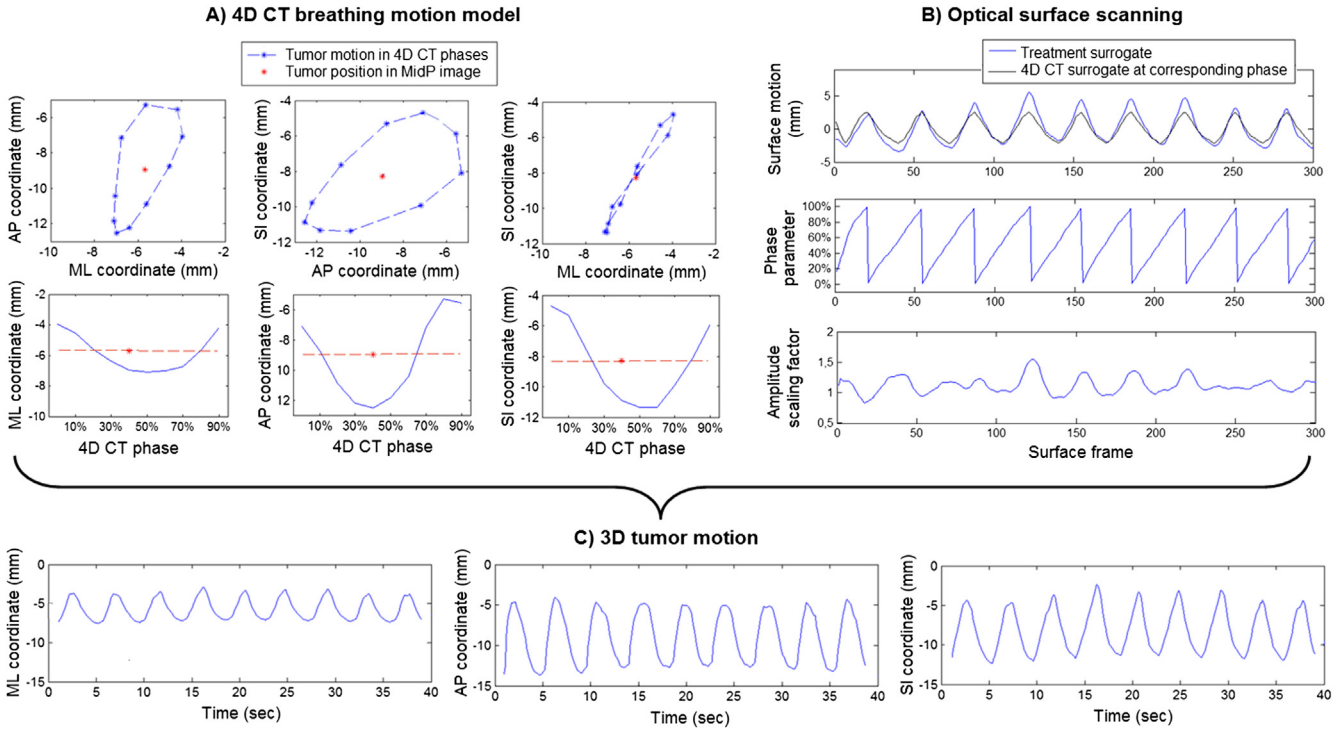

Fig. 2. A 4-dimensional (4D) computed tomography (CT) breathing motion model, defined by tumor centroid positions in the mid-position (MidP) image (baseline) and in each 4D CT phase volume. (B) Phase and amplitude parameters derived from the comparison between the breathing surrogates extracted from surface motion during treatment and during the 4D CT scan. (C) Tumor centroid trajectories estimated along the 3 spatial directions. AP = anteroposterior; ML = mediolateral; SI = superoinferior.

reference tumor motion identified in CBCT images was compared with the target trajectory estimated from the surrogate-driven motion model and projected on the 2-dimensional plane of the CBCT flat-panel detector, after correcting for the flex map values at different rotational angles (29).

Results

Table 1 lists for each patient the number of CBCT projections considered for the testing of the developed tumor tracking method, represented by the images acquired without surface occlusion in which lung lesion could be correctly identified. About 20-35 seconds of synchronized CBCT/GateCT acquisition could be analyzed per patient, corresponding on average to 7 breathing cycles. The absolute difference between the reference and estimated target trajectories are reported for all patients in Table 1. The median values of the tracking errors ranged between 0.7 and 2.2 mm for the horizontal image dimension, representing the projection of anteroposterior and mediolateral components of tumor motion, and between 1.2 and 2.4 mm for the vertical image dimension, corresponding to target motion projection along superoinferior direction. The exemplifying results on tumor motion tracking for 2 patients in the database are depicted in Figure 3. The developed tumor tracking method exhibited good performance, even in presence of breathing irregularities. As an example, despite the evident intercycle variations of the respiratory amplitude and phase parameters for patient P2 (Figure 3), the tumor trajectory estimated from external surface displacement correctly followed the reference target motion identified in CBCT projections, with median tracking errors of 1.7 and 1.2 mm for the horizontal and vertical directions, respectively (Table 1).

Figure 4 depicts for each patient the total tracking error in estimating tumor position in CBCT projections, computed as the root sum squared of the errors along the 2 image dimensions. To assess the effectiveness of the proposed respiratory modeling approach, based on phase, amplitude, and baseline parameters, the total error was also computed separating the contribution of each single parameter (Figure 4). The median value of the total errors computed over all patients was 5.4 mm when only the breathing phase was considered, setting to 1 the amplitude factor and taking as baseline the planning MidP CT image. These inaccuracies are partly associated with patient positioning errors, which have not

Table 1 Number of CBCT images considered per patient for the assessment of the tumor tracking accuracy, with the corresponding evaluated period of time and number of breathing cycles. The median values (25th-75th percentiles) of the absolute errors between the real and estimated tumor trajectories along the horizontal and vertical image directions are also reported in the table

Patient	No. of CBCT projections	Period of time (sec)	No. of breathing cycles	Horizontal tracking error (mm)	Vertical tracking error (mm)
P1	166	30.3	9	2.2 (1.2-3.8)	1.6 (0.9-2.7)
P2	175	31.9	5	1.7 (0.8-3.0)	1.2 (0.6-1.9)
P3	105	19.2	9	1.2 (0.6-1.7)	2.0 (1.6-2.4)
P4	189	34.5	8	0.7 (0.4-1.0)	1.4 (0.9-1.9)
P5	144	26.3	5	1.7 (0.8-3.1)	2.4 (1.4-3.5)
P6	159	29.0	6	1.3 (0.8-1.9)	1.5 (0.7-2.0)
P7	135	24.6	5	1.5 (0.9-2.3)	1.4 (0.6-2.2)

Abbreviation: CBCT = cone beam computed tomography.

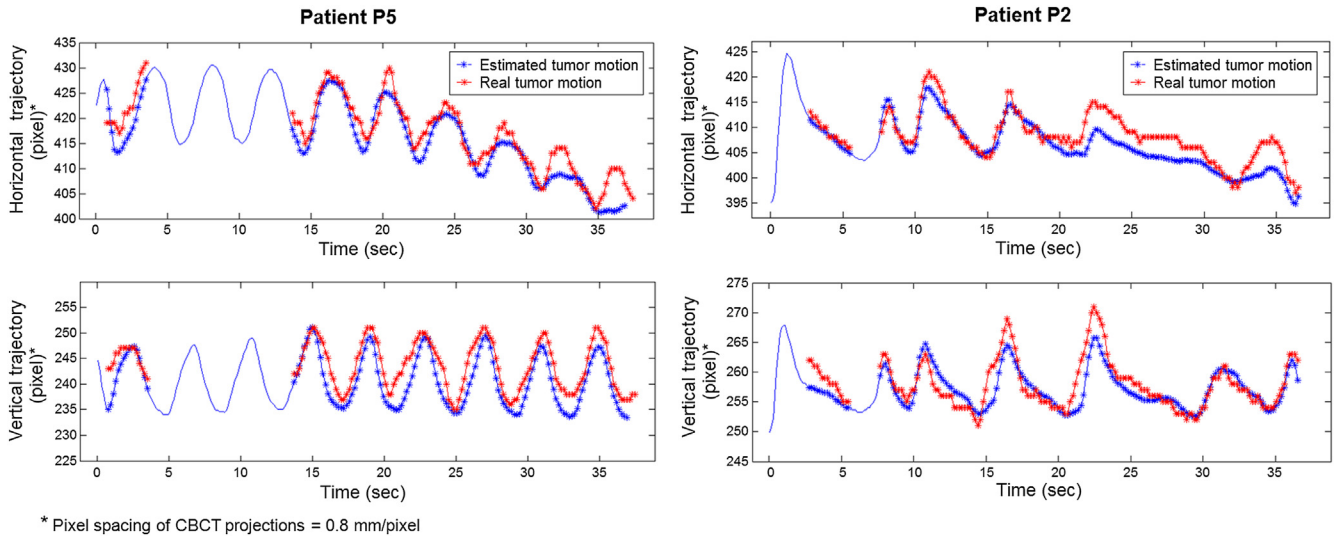

Fig. 3. Comparison between reference tumor trajectories identified in cone beam computed tomography (CBCT) projections along the horizontal and vertical image dimensions (red stars) and target trajectories estimated from surface motion and interpolated at the CBCT timestamps in which lung tumor was detectable (blue stars).

yet been compensated during the pretreatment CBCT scan. The median tumor tracking error was reduced to 2.6 mm after correcting for the baseline shifts between planning and treatment phases, and to 2.4 mm when also including the amplitude scaling factor. Except for patient P6, the baseline update allows a significant improvement of the tracking errors (Wilcoxon rank-sum test, $P < 0.05$). Instead, the introduction of amplitude correction did not significantly change the tracking results, although the total median error slightly decreased for 5 of 7 patients.

The residual influence of the different respiratory variables on tumor tracking accuracy when considering all 3 model parameters was also investigated. The following variables were computed for each complete respiratory cycle identified in the reference and estimated tumor trajectories:

- baseline, represented by the mean value of the tumor trajectory in the breathing cycle;
- amplitude, obtained from the difference between the maximum and minimum tumor coordinates in the cycle;
- period, estimated as the temporal difference between the 2 inspiratory peaks at the beginning and at the end of the cycle; and
- phase, computed as the mean acquisition timestamp of the 2 inspiratory peaks of the cycle, also expressed as percentage of the corresponding cycle period identified from CBCT images.

The median absolute difference between the reported respiratory variables computed for the reference and estimated breathing cycles along the horizontal and vertical image dimensions are reported in Table 2. The median errors of the cycle baseline and amplitude did not exceed 2.2 mm and 2.6 mm, respectively. The differences in the cycle periods varied from about 70 to 200 msec. The measured phase shifts were lower than 7% of the cycle length, corresponding to a maximum of 170 msec of delay. The linear correlation between the mean tracking errors associated to each identified cycle and the corresponding differences in the breathing variables was also computed. For 5 of 7 patients, the tracking errors proved to be correlated (Pearson coefficient > 0.8) with the baseline differences measured for tumor trajectories along at least 1 of the 2 spatial directions. Only for 1 patient we found a correlation between the tracking errors and the amplitude differences, whereas no correlation was measured for the phase and period variables.

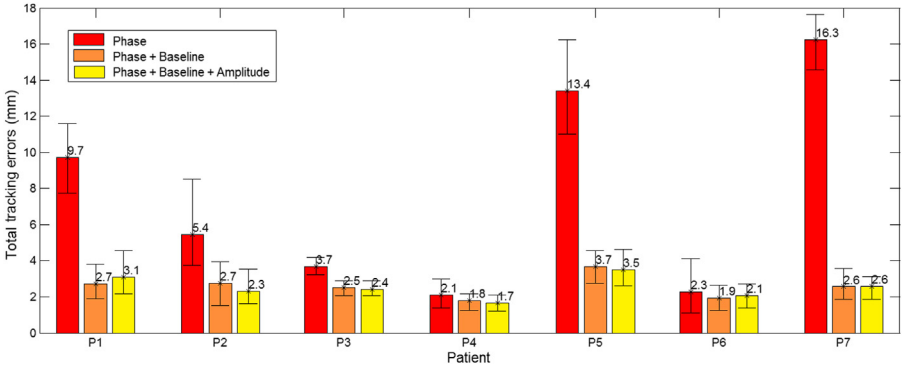

Fig. 4. Tumor tracking errors (median ± quartiles) obtained by considering only the phase parameter (red bars) and after introducing the baseline shift correction (orange bars) and the amplitude scaling factor (yellow bars).

Table 2 Median differences (25th-75th percentiles) between the respiratory variables computed for each breathing cycle identified on the real and estimated tumor trajectories

Patient	Baseline error (mm)	Amplitude error (mm)	Period error (msec)	Phase error (msec)	Percentage phase error (%)
P1	1.6 (0.7-2.0)	1.3 (0.7-3.9)	130 (49-213)	110 (73-216)	2.9 (1.5-5.9)
P2	0.7 (0.5-1.3)	2.6 (0.9-4.7)	129 (80-231)	70 (40-130)	1.0 (0.4-1.9)
P3	1.7 (0.7-2.0)	1.0 (0.3-1.4)	71 (16-190)	111 (85-235)	6.7 (3.9-14.0)
P4	0.8 (0.1-1.5)	1.7 (0.9-2.0)	170 (73-213)	136 (69-274)	3.3 (0.7-4.8)
P5	2.2 (1.3-2.6)	0.9 (0.5-1.9)	203 (73-370)	170 (69-285)	3.7 (1.8-4.0)
P6	1.2 (0.8-1.5)	1.0 (0.4-1.8)	74 (41-272)	107 (34-270)	2.7 (1.2-4.7)
P7	1.2 (0.9-2.0)	1.2 (1.1-2.6)	198 (95-254)	156 (89-279)	5.7 (4.5-6.1)

Discussion

A novel approach for the indirect tracking of intrafraction moving tumors was proposed and investigated, exploiting a patient-specific motion model derived from time-resolved planning CT and driven during treatment by an external surrogate obtained from noninvasive optical surface imaging. The experimental testing was based on real clinical CBCT data acquired from lung cancer patients. Although the proposed method allows estimating tumor motion along all 3 spatial directions, as shown in Figure 2c, the tracking accuracy could be quantified only in 2 dimensions, represented by the horizontal and vertical axes of the CBCT imager panel (Figure 3). However, the greatest amplitude of lung tumor motion is generally found in the superoinferior direction (1), which is visible on the vertical axis regardless of the panel rotational position. An average tracking error of 1.5 mm was measured along each image dimension, which is comparable to the state-of-the-art tracking techniques currently applied in conventional x-ray radiation therapy (13-15). The obtained error can be partly associated to the inaccuracies in localizing lung lesions in CBCT projections, featuring an intrinsic spatial resolution of 0.8 mm/pixel. The measured shifts in the identification of the breathing phase can be partly related to the temporal resolution of CBCT scans, requiring about 180 msec for the acquisition of a single projection.

In most patients in the database, tumor tracking inaccuracies proved to be correlated to errors in the estimation of the breathing baseline, for which only interfraction variations are compensated in the present approach. In particular, baseline shift corrections are estimated by nonrigidly registering the noise-free MidP CT image with the free-breathing CBCT volume, which is affected by blurring from breathing motion. A possible improved solution might be the use of a motion-compensated CBCT with image-blur reduction (18) for baseline correction. Another future development can be represented by the introduction of intrafraction baseline updates, by retrieving its instantaneous values from the surface-based surrogate signal, as currently performed for the breathing amplitude and phase parameters. Major concerns are associated with the computational cost of the developed tumor tracking algorithm, which does not currently provide real-time performance. The most time-consuming process is represented by the deformable mesh registration algorithm (23), which can, however, be optimized based on the work proposed elsewhere (30), demonstrating the feasibility of a real-time nonrigid surface registration.

Surrogate-driven motion models built from Cine-CT or CBCT data have already been proposed for tumor tracking applications (21, 31, 32). Differently from the method developed previously (32) based on rigid-translation motion models, we employed a nonrigid deformation-based approach that allows accounting not only for tumor motion but for the entire patient anatomy. We also introduced specific strategies to compensate for the day-to-day variations in the respiratory motion parameters, which are not taken into account in the modeling approach proposed previously (31, 32). In particular, amplitude changes are compensated though a scaling factor obtained by comparing motion amplitudes during planning and treatment phases. Baseline shifts are corrected using deformable registration, which can potentially improve the tracking accuracy in different lung regions with respect to the rigid alignment performed previously (21). The effectiveness of the proposed respiratory modeling approach was demonstrated on the tested data. As depicted in Figure 4, the use of only the breathing phase parameter led to tumor tracking errors up to 16.3 mm, which were significantly reduced by the introduction of the baseline update and slightly further decreased by including also the amplitude scaling factor.

The proposed tumor tracking method provides substantial benefits with respect to the state-of-the-art technique based on external−internal correlation models (12-15). The presented approach exploits the anatomical, motion-correlated information provided by the 4D planning CT through a patient-specific adaptive motion model, which is combined to the noninvasive optical imaging of patient surface at the time of treatment for the update of breathing parameters. Although an x-ray-based assessment of the reliability of the motion model is envisaged, our technique does not involve the estimation and frequent verification of external−internal correlation parameters by means of repeated radiographs, thus requiring a less intense use of in-room invasive imaging. Only an initial CBCT scan, which is already commonly acquired for patient setup, is needed for interfraction baseline corrections. In addition, the developed approach does not require implanted fiducial clips, neither in case of low-contrast lesions such as liver or lung cancers, thus avoiding possible drawbacks associated to clip implantation, such as the risk of pneumothorax or fiducial migration (33).

Differently from the current marker-based applications employing a limited number of surface fiducial points (12-15), the proposed tumor tracking method makes use of the redundant motion information of the entire thoracoabdominal surface provided by markerless imaging systems. This allows capturing the complex and detailed aspects of the different breathing patterns involved in external surface motion, overcoming also the issue related to the variation of external−internal correlation from marker locations on the patient surface (34, 35). Moreover, current correlation-based tracking techniques only allow predicting the position of single internal points from the external surrogate.

Conversely, our approach can be potentially extended to track the entire patient anatomy included in the CT scan, thus providing the daily dynamics because of breathing motion of all structures and organs at risk in the thoracoabdominal region. This information can be particularly useful in particle therapy for obtaining the density and radiological variations of beam path length associated to organ motion, required to adapt the depth range of particle beams (36).

References

1. Keall PJ, Mageras GS, Balter JM, et al. The management of respiratory motion in radiation oncology report of AAPM Task Group 76. *Med Phys* 2006;33:3874-3900.
2. Bert C, Durante M. Motion in radiotherapy: Particle therapy. *Phys Med Biol* 2011;56:R113-R144.
3. Schweikard A, Shiomi H, Adler J. Respiration tracking in radiosurgery. *Med Phys* 2004;31:2738-2741.
4. Poulsen PR, Cho B, Sawant A, et al. Dynamic MLC tracking of moving targets with a single kV imager for 3D conformal and IMRT treatments. *Acta Oncol* 2010;49:1092-1100.
5. Richter A, Wilbert J, Baier K, et al. Feasibility study for markerless tracking of lung tumors in stereotactic body radiotherapy. *Int J Radiat Oncol Biol Phys* 2010;78:618-627.
6. Baroni G, Riboldi M, Spadea MF, et al. Integration of enhanced optical tracking techniques and imaging in IGRT. *J Radiat Res* 2007;48:A61-A74.
7. Bert C, Metheany KG, Doppke K, et al. A phantom evaluation of a stereo-vision surface imaging system for radiotherapy patient setup. *Med Phys* 2005;32:2753-2762.
8. Seregni M, Pella A, Riboldi M, et al. Real-time tumor tracking with an artificial neural networks-based method: A feasibility study. *Phys Med* 2011;. http://dx.doi.org/10.1016/j.ejmp.2011.11.005.
9. Berbeco RI, Nishioka S, Shirato H, et al. Residual motion of lung tumors in end-of-inhale respiratory gated radiotherapy based on external surrogates. *Med Phys* 2006;33:4149-4156.
10. Schweikard A, Glosser G, Bodduluri M, et al. Robotic motion compensation for respiratory movement during radiosurgery. *Comput Aided Surg* 2000;5:263-277.
11. Kamino Y, Takayama K, Kokubo M, et al. Development of a four-dimensional image-guided radiotherapy system with a gimbaled x-ray head. *Int J Radiat Oncol Biol Phys* 2006;66:271-278.
12. Kilby W, Dooley JR, Kuduvalli G, et al. The CyberKnife Robotic Radiosurgery System in 2010. *Technol Cancer Res Treat* 2010;9:433-452.
13. Hoogeman M, Prevost JB, Nuyttens J, et al. Clinical accuracy of the respiratory tumor tracking system of the Cyberknife: Assessment by analysis of log files. *Int J Radiat Oncol Biol Phys* 2009;74:297-303.
14. Pepin EW, Wu H, Zhang Y, et al. Correlation and prediction uncertainties in the CyberKnife Synchrony respiratory tracking system. *Med Phys* 2011;38:4036-4044.
15. Torshabi AE, Pella A, Riboldi M, et al. Targeting accuracy in real-time tumor tracking via external surrogates: A comparative study. *Technol Cancer Res Treat* 2010;9:551-562.
16. Wolthaus JWH, Sonke JJ, van Herk M, et al. Reconstruction of a time-averaged midposition CT scan for radiotherapy planning of lung cancer patients using deformable registration. *Med Phys* 2008;35:3998-4011.
17. McClelland JR, Blackall JM, Tarte S, et al. A continuous 4D motion model from multiple respiratory cycles for use in lung radiotherapy. *Med Phys* 2006;33:3348-3358.
18. Rit S, Wolthaus JWH, van Herk M, et al. On-the-fly motion-compensated cone-beam CT using an a priori model of the respiratory motion. *Med Phys* 2009;36:2283-2296.
19. Vandemeulebroucke J, Kybic J, Clarysse P, et al. Respiratory motion estimation from cone-beam projections using a prior model. *Med Image Comput Comput Assist Interv* 2009;12:365-372.
20. Shackleford JA, Kandasamy N, Sharp GC. On developing B-spline registration algorithms for multi-core processors. *Phys Med Biol* 2010;55:6329-6351.
21. McClelland JR, Hughes S, Modat M, et al. Interfraction variations in respiratory motion models. *Phys Med Biol* 2011;56:251-272.
22. Sonke JJ, Lebesque J, van Herk M. Variability of four-dimensional computed tomography patient models. *Int J Radiat Oncol Biol Phys* 2008;70:590-598.
23. Schaerer J, Fassi A, Riboldi M, et al. Multi-dimensional respiratory motion tracking from markerless optical surface imaging based on deformable mesh registration. *Phys Med Biol* 2012;57:357-373.
24. Gianoli C, Riboldi M, Spadea MF, et al. A multiple points method for 4D CT image sorting. *Med Phys* 2011;38:656-667.
25. Britton KR, Starkschall G, Tucker SL, et al. Assessment of gross tumor volume regression and motion changes during radiotherapy for non-small-cell lung cancer as measured by four-dimensional computed tomography. *Int J Radiat Oncol Biol Phys* 2007;68:1036-1046.
26. Gabor D. Theory of communications. *J Inst Electric Engin* 1946;93:429-457.
27. Fassi A, Schaerer J, Riboldi M, et al. A novel CT-based contrast enhancement technique for markerless lung tumor tracking in X-ray projection images. *Radiother Oncol* 2011;99:S217.
28. Yang Y, Zhong Z, Guo X, et al. A novel markerless technique to evaluate daily lung tumor motion based on conventional cone-beam CT projection data. *Int J Radiat Oncol Biol Phys* 2012;82:e749-e756.
29. Bissonnette JP, Moseley D, White E, et al. Quality assurance for the geometric accuracy of cone-beam CT guidance in radiation therapy. *Int J Radiat Oncol Biol Phys* 2008;71:S57-S61.
30. Wasza J, Bauer S, Hornegger J. Real-time motion compensated patient positioning and non-rigid deformation estimation using 4-D shape priors. *Med Image Comput Assist Interv* 2012;15:576-583.
31. Fayad H, Pan T, Pradier O, Visvikis D. Patient specific respiratory motion modeling using a 3D patient's external surface. *Med Phys* 2012;39:3386-3395.
32. Martin J, McClelland J, Yip C, et al. Building motion models of lung tumours from cone-beam CT for radiotherapy applications. *Phys Med Biol* 2013;58:1809-1822.
33. Nelson C, Starkschall G, Balter P, et al. Assessment of lung tumor motion and setup uncertainties using implanted fiducials. *Int J Radiat Oncol Biol Phys* 2007;67:915-923.
34. Koch N, Liu HH, Starkschall G, et al. Evaluation of internal lung motion for respiratory-gated radiotherapy using MRI: Part I-correlating internal lung motion with skin fiducial motion. *Int J Radiat Oncol Biol Phys* 2004;60:1459-1472.
35. Gierga DP, Brewer J, Sharp GC, et al. The correlation between internal and external markers for abdominal tumors: implications for respiratory gating. *Int J Radiat Oncol Biol Phys* 2005;61:1551-1558.
36. Riboldi M, Orecchia R, Baroni G. Real-time tumour tracking in particle therapy: technological developments and future perspectives. *Lancet Oncol* 2012;13:e383-e391.